Landslides in Belgium—Two Case Studies in the Flemish Ardennes and the Pays de Herve

20

Olivier Dewitte, Miet Van Den Eeckhaut, Jean Poesen and Alain Demoulin

Abstract

Most landslides in Belgium, and especially the largest features, do not occur in the Ardenne, where the relief energy and the climate conditions seem most favourable. They appear in regions located mainly north of them where the lithology consists primarily of unconsolidated material. They develop on slopes that are relatively smooth, and their magnitude is pretty large with regard to that context. An inventory of more than 300 pre-Holocene to recent landslides has been mapped. Twenty-seven percent of all inventoried landslides are shallow complex landslides that show signs of recent activity. The remaining landslides are deep-seated features and rotational earth slides dominate ($n > 200$). For such landslides, the average area is 3.9 ha, but affected areas vary from 0.2 to 40.4 ha. The exact age of the deep-seated landslides is unknown, but it is certain that during the last century no such landslides were initiated. Both climatic and seismic conditions during the Quaternary may have triggered landslides. The produced landslide inventory is a historical inventory containing landslides of different ages and triggering events. Currently, only new shallow landslides or reactivations within existing deep-seated landslides occur. The focus on the Hekkebrugstraat landslide in the Flemish Ardennes allows us to understand the recent dynamics of a large reactivated landslide. It shows the complexity of the interactions between natural and human-induced processes. The focus on the Pays the Herve allows for a deeper understanding of landslide mechanisms and the cause of their origin in natural environmental conditions. These two examples are among the best-studied landslides and their analysis allows us to highlight the main processes at play and to better unravel their interactions.

Keywords

Mass movement • Flemish Ardennes • Pays de Herve • Landslide reactivation • Landslide cause • Triggering factors

O. Dewitte (✉)
Department of Earth Sciences, Royal Museum for Central Africa, Leuvensesteenweg 13, 3080 Tervuren, Belgium
e-mail: olivier.dewitte@africamuseum.be

M. Van Den Eeckhaut
Arcadis Belgium, Koningsstraat 80, 1000 Brussels, Belgium
e-mail: miet.vandeneeckhaut@arcadis.com

J. Poesen
Department of Earth and Environmental Sciences, KU Leuven, Celestijnenlaan 200E, 3001 Leuven-Heverlee, Belgium
e-mail: jean.poesen@kuleuven.be

A. Demoulin
Department of Physical Geography and Quaternary, University of Liège, Sart Tilman, B11, 4000 Liège, Belgium
e-mail: ademoulin@ulg.ac.be

A. Demoulin (ed.), *Landscapes and Landforms of Belgium and Luxembourg*, World Geomorphological Landscapes, DOI 10.1007/978-3-319-58239-9_20

20.1 Introduction

At the European level, Belgium does not appear as a country prone to landsliding (Günther et al. 2014). Topographic conditions such as those found in mountain environments are not present and processes capable of triggering landslides, whether seismic or climatic, occur very rarely. Therefore, large slope instabilities, such as those found in the Alps for instance (Crosta et al. 2013), are not observed. However, an interesting point about landslide processes in Belgium is that most instabilities, and especially the largest ones, do not occur in the Ardenne where the relief energy and the climate conditions are the most favourable. They appear in regions located mainly north of them, on slopes that are relatively smooth, and their magnitude is pretty large with regard to that context (Fig. 20.1). The objective of this chapter is to provide a general picture of the landslides in these regions and then to focus on two representative cases. These two examples are among the best-studied landslides in Belgium and their understanding allows for highlighting the main processes at play and better unravelling their interactions.

20.2 Landslides in Middle Belgium

20.2.1 Geographical and Geological Settings

The Flemish hills located in Southern Flanders are clearly marked by landslide processes (Fig. 20.2). The 4850 km^2 area of Southern Flanders contains five hilly regions where slope angles are often steeper than 3° (Fig. 20.2a). From west to east these are the West Flemish hills (up to 155 m asl), the hills of the Flemish Ardennes (up to 156 m asl), the Pajottenland hills (up to 112 m asl), the Hageland hills (up to 105 m asl) and the Haspengouw hills (up to 128 m asl). These hilly regions are separated by wide valleys of the Leie, Scheldt, Dender, Dijle and Gete rivers (Fig. 20.2). The lithology consists primarily of unconsolidated Late Miocene to Early Palaeocene sediments, with some west–east

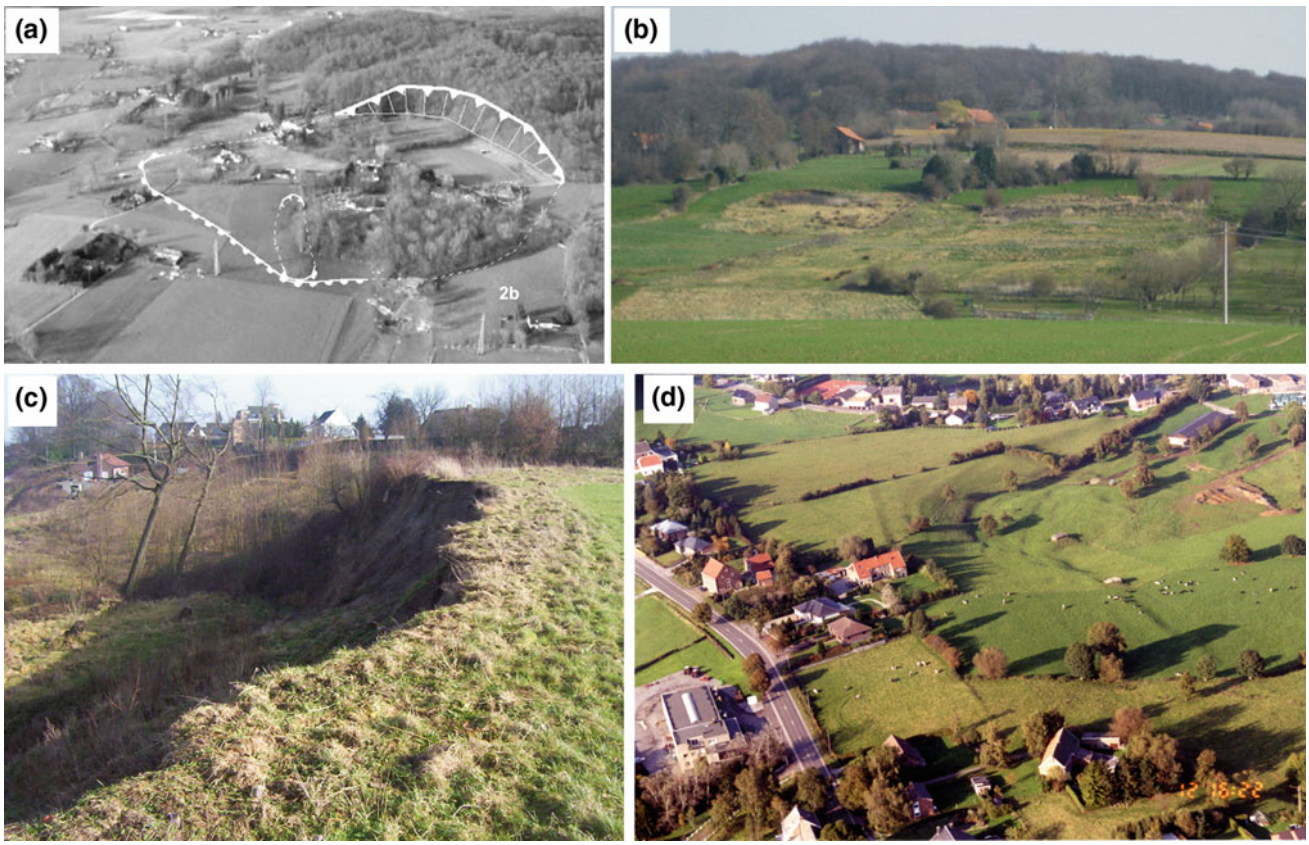

Fig. 20.1 Landslide examples in Middle Belgium and Pays de Herve. **a** Typical large deep-seated landslide in the Flemish Ardennes (Wittentak, March 2004, photo by J. Poesen in Van Den Eeckhaut et al. 2005). The *white lines* represent the limits of the landslide: main scarp (*right*) and toe (*left*). See Fig. 20.2f for location. **b** Frontal view of two adjacent shallow complex slides located in the West Flemish hills (Dranouter landslide, March 2009, photo by M. Van Den Eeckhaut in Van Den Eeckhaut et al. 2011). See Fig. 20.2d for location. **c** Main scarp of an old deep-seated landslide reactivated in March 2001 (Maarkedal, February 2003, photo by O. Dewitte in Dewitte 2006). See Fig. 20.2f for location. **d** Middle-sized deep-seated landslide in the Pays de Herve (Chaineux, 1999, photo by A. Pissart). See Fig. 20.10 or location

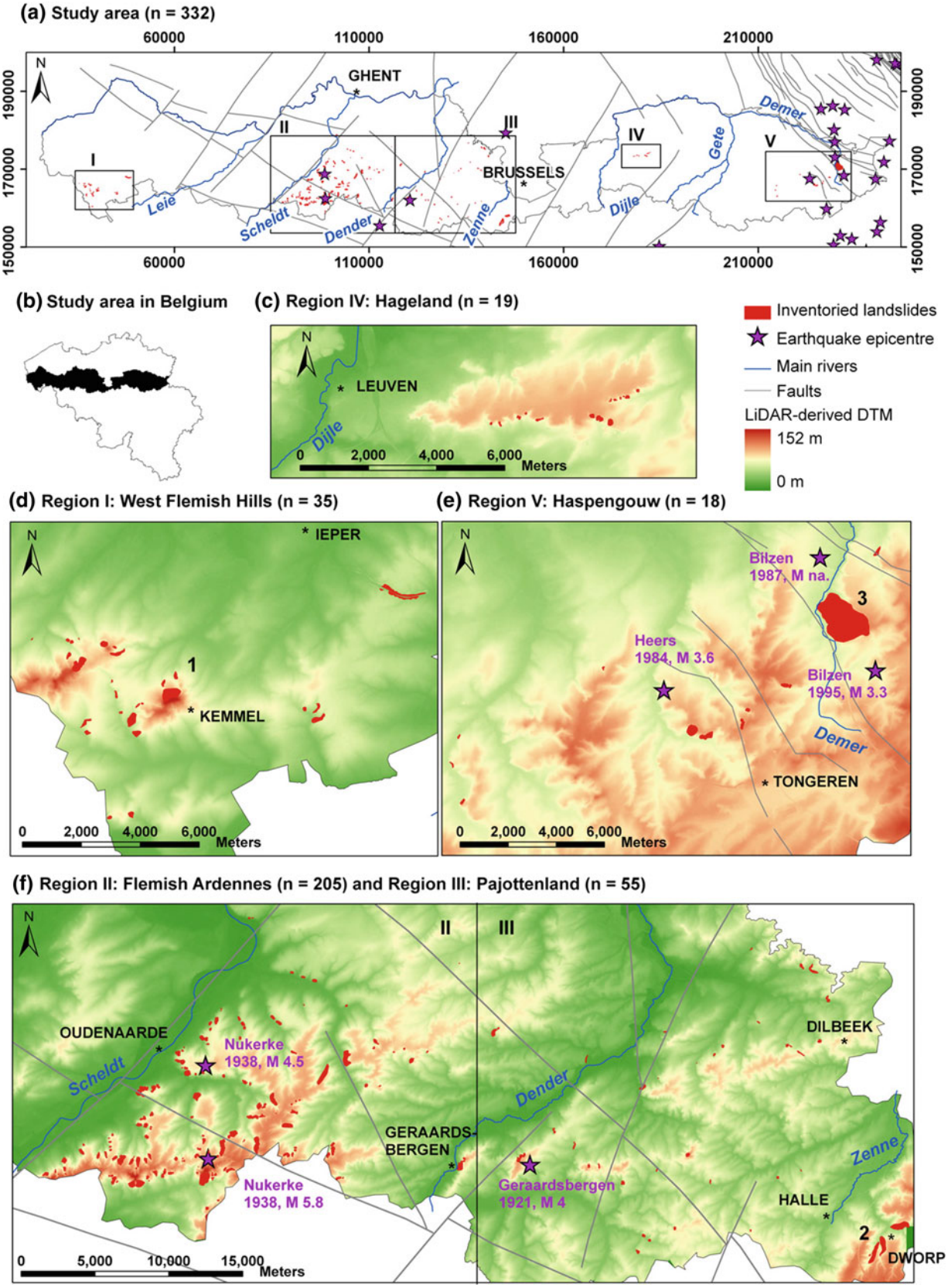

Fig. 20.2 **a** Regions in Southern Flanders (Middle Belgium) where landslides have been mapped (Belgian Lambert 72 coordinates in m). **b** Location of the represented areas within Belgium. **c** Landslides in Hageland. **d** Landslides in the West Flemish hills. **e** Landslides in Haspengouw. **f** Landslides in the Flemish Ardennes and Pajottenland. Excerpts from the Flemish LiDAR DTM (from Van Den Eeckhaut et al. 2011)

variability in the distribution of the lithostratigraphic units. These Cenozoic formations consist of subhorizontal layers of alternating sand, clay and clay-silt dipping at 0.2° towards the northeast (Jacobs et al. 1999).

Analysis of LiDAR-derived imagery (shaded relief, slope, surface roughness and contour maps) combined with intense field work led to the discovery of more than 330 old and recent large landslides in the region (Van Den Eeckhaut et al. 2007b, 2011) (Figs. 20.2 and 20.3). The Flemish Ardennes (Fig. 20.2f) is the region where a majority of the landslides (more than 200) was observed. In the field, all landslides were classified according to Cruden and Varnes (1996). Based on field estimate of the depth of the surface of rupture, landslides with a surface of rupture deeper than 3 m, but generally deeper than 10 m, and landslides with this surface at a depth of less than 3 m were classified as deep-seated and shallow, respectively. Deep-seated rotational earth slides dominate, accounting for 65% (n = 217) of the mapped landslides (Van Den Eeckhaut et al. 2011). Eight percent of the deep-seated movements are classified as complex. Twenty-seven percent (n = 90) of all inventoried landslides are shallow complex landslides (Fig. 20.1b). For about 50 of them, detailed information on the initiation or reactivation date was found (Van Den Eeckhaut et al. 2011). With the exception of four landslide events reported between AD 1828 and AD 1926, all dated historical landslide events occurred after AD 1960. Moreover, many of the remaining undated shallow landslides show signs of recent activity (Van Den Eeckhaut et al. 2011).

There is a high degree of variability in the metrics of individual slides in each landslide type (Van Den Eeckhaut et al. 2011). The smallest shallow landslide identified has a landslide-affected area of 0.5–0.75 ha. The mean area of deep-seated rotational earth slide is 3.9 ha, but area varies from 0.2 to 40.4 ha, similar to the range shown by deep-seated complex slides. Most landslides have mean slope gradients in the order of 10–11°. Susceptibility analyses for deep-seated landslides in the Flemish Ardennes show that slope gradient and lithology are the controlling factors with the highest predictive power (Van Den Eeckhaut et al. 2006, 2009b).

To complete the picture, it is worth mentioning that two landslides in Haspengouw (Fig. 20.2e) were classified as deep-seated gravitational slope deformations (DSGSDs), i.e. mass movement defined to affect an entire slope and be generated by mechanical processes such as deep-seated block sliding and lateral spreading (Van Den Eeckhaut et al. 2011). The Alden Biesen DSGSD (nr. 3 in Fig. 20.2e) is located in the eastern part of Flanders near the town of Bilzen. With an area of 266.5 ha, it is the largest landslide in Southern Flanders, being significantly larger than the second largest form in the region (i.e. the 42.0 ha Muziekberg landslide in the Flemish Ardennes). With the exception of the Kolmont landslide (7.0 ha) located less than 10 km southwest of Alden Biesen, no other DSGSD was found in Southern Flanders (Van Den Eeckhaut et al. 2011).

The exact age of the deep-seated landslides is unknown, but it is certain that during the last century no such landslides

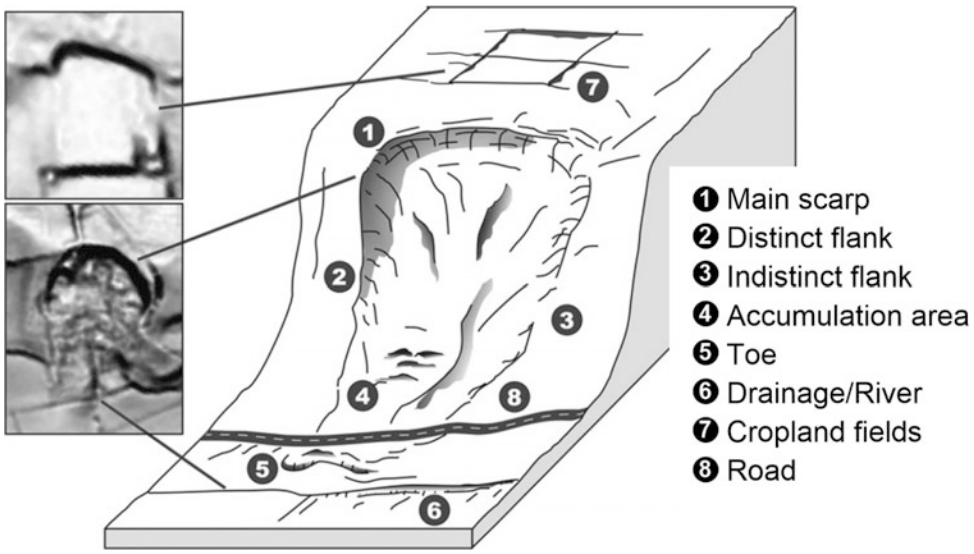

Fig. 20.3 Sketch of a typical landslide in its typical physical environment in the Flemish hills, with excerpts of the LiDAR-derived shaded relief map illustrating two characteristic topographic features of the study area, namely a cropland field with earth banks, or lynchets (*top left*) and the main scarp of a deep-seated landslide (*bottom left*). This conceptualization is also valid for the Pays the Herve where landslide features are very similar (see Fig. 20.11). Landslide features are defined according to IAEG Commission on Landslides (1990) (from Van Den Eeckhaut et al. 2012)

were initiated (Ost et al. 2003; Van Den Eeckhaut et al. 2005, 2011). Only one study in the Flemish Ardennes attempted to unravel the age and history of an old landslide and obtained an AMS ^{14}C age of 8700–8440 cal year BP that dates the Collinabos landslide to the beginning of the Boreal (Van Den Eeckhaut et al. 2007c). This corresponds to a relatively wet period coinciding with permafrost melting (Van Den Eeckhaut et al. 2011) and it is likely that other landslides were initiated in Flanders during this period. However, the subdued topography of some landslides, especially the DSGSDs, suggests they may be pre-Holocene (Van Den Eeckhaut et al. 2011).

Apart from a climatic trigger, the possibility of a seismic origin of the landslides has been evoked as the highest landslide densities often coincide with the presence of Quaternary active faults (Fig. 20.2a; Ost et al. 2003; Van Den Eeckhaut et al. 2011). Indeed, the many landslides of the Flemish Ardennes concentrate in an area where two earthquakes occurred during the twentieth century, the Geraardsbergen 1921 ($M_L = 4$) and Nukerke 1938 ($M_L = 5.8$) earthquakes (Fig. 20.2f), and where Camelbeeck (1993) locates the seismogenic South Brabant Fault Zone. Although Somville (1939) reported that the 1938 earthquake had an important impact on the groundwater flow, forming new springs and relocating existing ones, no historical document linking landslide activity to earthquakes has been found.

Both climatic and seismic conditions during the Quaternary may have caused landslides in Southern Flanders. The landslide inventory is a historical inventory containing landslides of different ages and triggering events. Currently, only new shallow landslides or reactivations within existing deep-seated landslides occur in the study area (Ost et al. 2003; Dewitte et al. 2008, 2009; Van Den Eeckhaut et al. 2009a, 2011). Despite their relatively small displacement distances, these movements are a continuously operating process causing considerable economic damage (Vranken et al. 2013). In the Flemish Ardennes alone, the annual landslide risk is estimated to vary between 51 and 86 million € (2011 values; Vranken et al. 2014). Note that the inventory of Southern Flanders, as other historical inventories, is assumed to be incomplete as morphological characteristics of old shallow landslides can be obliterated by human activities (e.g. land levelling) and soil erosion (see Chap. 15) or hidden by dense vegetation (Van Den Eeckhaut et al. 2007a).

20.2.2 Sixty-Five Years of Slope Movements Documented in the Flemish Ardennes: The Hekkebrugstraat Landslide

As stated above, large deep-seated landslides in the Flemish Ardennes occurred in an undefined epoch far before present time and due to specific environmental conditions. In contrast, observation of their current activity strongly suggests that the most probable mass movement hazard in these regions is actually not the occurrence of new such landslides but reactivation of the pre-existing ones (Dewitte and Demoulin 2005; Dewitte et al. 2006, 2008, 2009, 2010).

Located on the Leupegem hill, Flemish Ardennes, next to the town of Oudenaarde (Landslide 1, Fig. 20.4), the Hekkebrugstraat landslide (HL) is a representative example of these deep-seated rotational earth slides. It suffered a deep reactivation in 1995 that caused ground displacements of several metres. Eyewitness reports of its evolution since the 1950s as well as of various human activities within and near the landslide have been documented by Van Den Eeckhaut et al. (2007a). In addition, quantitative estimates of the displacements have been obtained for the period 1952–2002 (Dewitte et al. 2008, 2009). This well-documented landslide thus allows for unravelling the processes that drive its present activity.

The HL dimensions are typical of those of other landslides in the Flemish hills. It extends over an area of ca. 9 ha, has a total length of 370 m, and a maximum width of 260 m. The maximum height of its main scarp is 9 m. The HL cuts across the Aalbeke Member of the Kortrijk Formation, which consists of 10-m-thick homogeneous blue massive clays highly sensitive to landsliding (Van Den Eeckhaut et al. 2006, 2009b, 2011).

20.2.2.1 Insights from Archives and Eyewitness Reports

Although the emphasis is put on the HL history since the 1950s, a short overview of the information on both the landslide and land use prior to 1945 is relevant. For this purpose, two historical maps, the Ferraris map of 1771 (Fig. 20.5a) and a map from 'The atlas of the rural roads' (1841) were analysed (Van Den Eeckhaut et al. 2007a). There is no indication of a landslide on the Ferraris map (Fig. 20.5a). At the end of the eighteenth century, the area currently affected by the landslide was forested, while the upslope contributing area was under cropland or pasture. The fact that the Hekkebrug road is indicated by a thick brown line on the Ferraris map suggests that the road was a sunken lane, and that the hillslope was well drained, preventing topsoil saturation. Despite the absence of the HL on the Ferraris map, there are four reasons to believe that the hillslope had already failed at that time. The first is that none of the other large landslides mapped in the Flemish Ardennes are shown on this map. Second, there is a lack of historical documents describing the initiation of the landslide after the eighteenth century. As it is located only 2 km from the city of Oudenaarde (Fig. 20.4), and as there were already six houses within less than 500 m of the present-day landslide in 1771 (Fig. 20.5a), it seems very unlikely that the initiation would have post-dated 1771 without having been

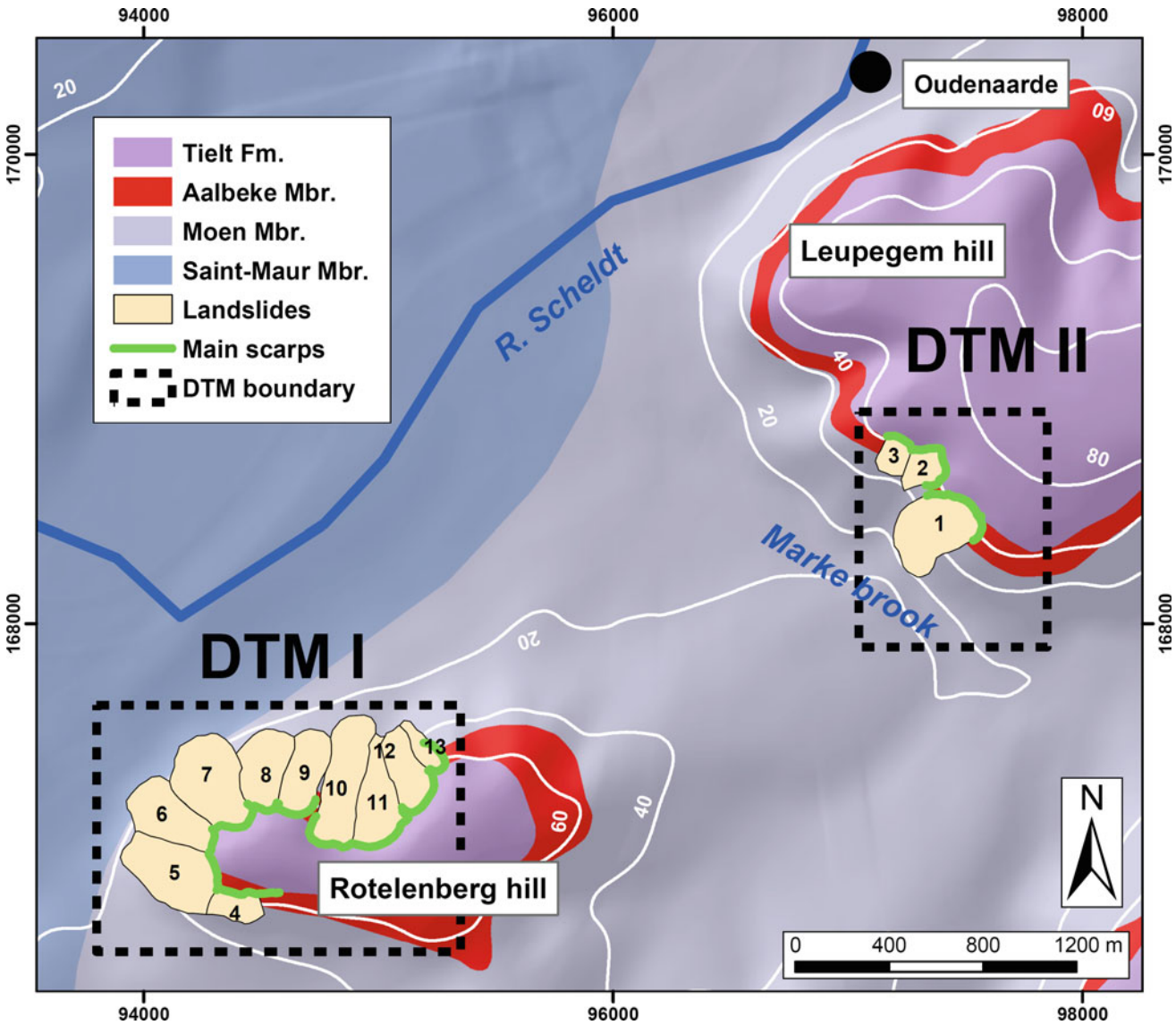

Fig. 20.4 Location map of the Hekkebrugstraat landslide (landslide 1 in the figure) and the surrounding landslides with the lithological and topographic context. The landslides are located next and south of the town of Oudenaarde (see Fig. 20.2f for general location). The scars and the main scarps of the landslides are superposed on the regional geology (Eocene). The quadrangles DTM I and DTM II locate the Digital Terrain Models used for ground displacement measurements within the 13 landslides (see Dewitte et al. 2008, 2009 for additional information). In this chapter, only ground displacements for landslide 1 are shown (Figs. 20.7 and 20.8). The altitudes (*white contour lines*) and coordinates (Belgian Lambert 72) are in metres (from Dewitte et al. 2010)

reported. The third reason is that, in contrast to most surrounding hillslope sections, which were used as either cropland or pasture, the HL site itself was forested. This strongly suggests that the microtopographical and/or hydrological conditions of the site were not suitable for agricultural activities. Finally, the curved shape of the path leading to the farm, superposed to the present position of the landslide scarp, was most probably imposed by an existing slope discontinuity. The map from 'The atlas of the rural roads' (1841) only shows roads and field plots. The curved shape of both the plots downslope and the footpath upslope of the present-day main scarp location again indicate the presence of a break in the slope pointing to a pre-existing slope failure. The slipped area was at least partly cultivated in the mid-nineteenth century, as the depletion zone was divided into small plots.

From 1950, more detailed information is available from aerial photographs and interviews with local inhabitants (Van Den Eeckhaut et al. 2007a). Undoubtedly, there was a landslide, and the affected area was partly cultivated (Fig. 20.5b). From 1952 (Fig. 20.5b) to 1996 (Fig. 20.5c), land-use changes are obvious. They are explained by several

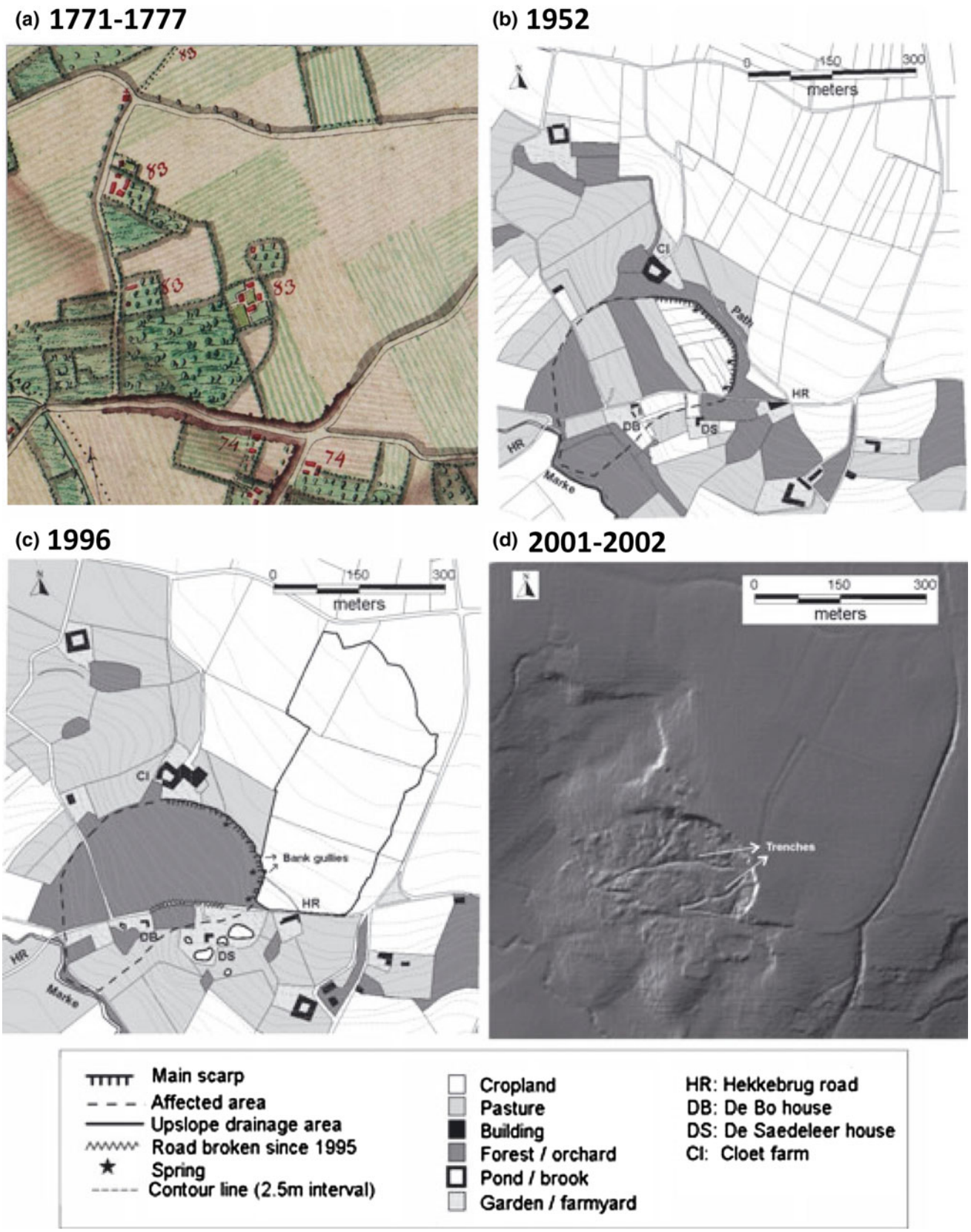

Fig. 20.5 Evolution of the Hekkebrugstraat landslide site as revealed by old maps. **a** Excerpt of the Ferraris map (1771–1777). **b** Situation around 1952 based on aerial photograph interpretation. **c** Situation around 1996 based on aerial photograph interpretation. **d** Topography around 2001–2002 shown on a LIDAR-derived hillshade map (DEM of Flanders 2007) (from Van Den Eeckhaut et al. 2007a)

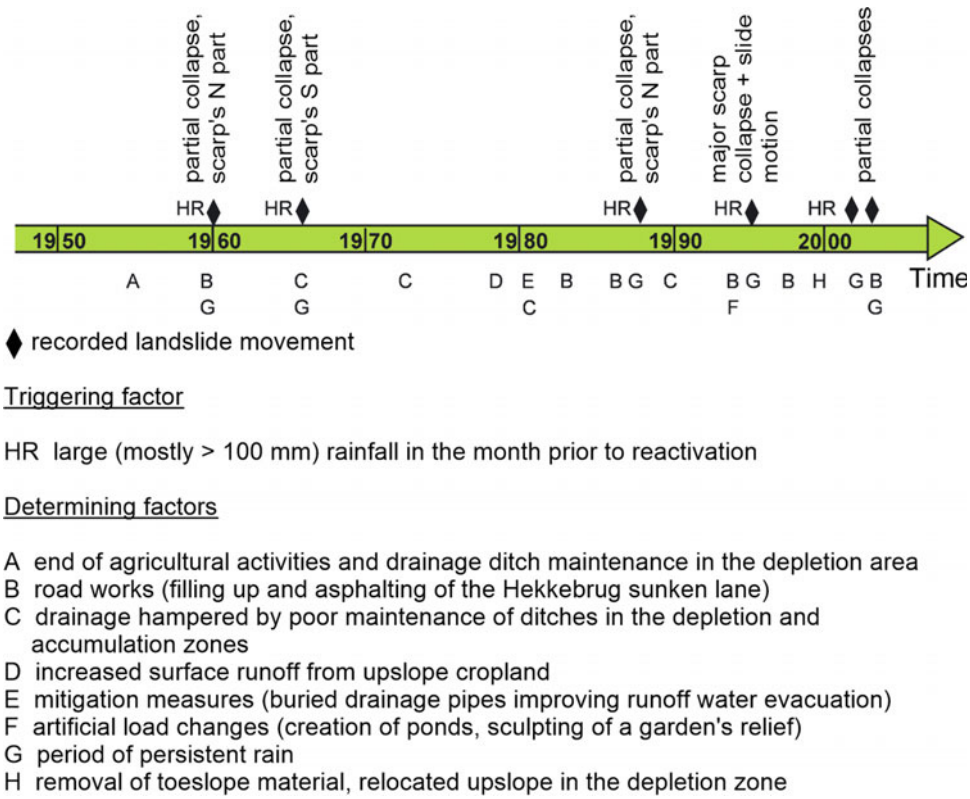

Fig. 20.6 Inventory of the determining and triggering factors responsible for reactivations of the Hekkebrugstraat landslide from the 1950s to 2005 (from Van Den Eeckhaut et al. 2007a)

natural and anthropogenic factors reported by Van Den Eeckhaut et al. (2007a) and summarized in Fig. 20.6. Since 1950, movements of HL have occurred at least six times. The reactivation of 1995 was the most catastrophic. Most displacements occurred after monthly rainfall depths above 100 mm during the previous months. Long periods of high rainfall, and the presence of relatively steep slopes, impermeable clays and springs are important natural causal factors. Equally important, however, are anthropogenic determining factors (Van Den Eeckhaut et al. 2007a). The information collected by Van Den Eeckhaut et al. (2007a) is of primary importance for the validation of the landslide displacements analysed below.

20.2.2.2 Vertical Displacements

The understanding of landslide mechanisms is greatly facilitated when accurate quantitative information on their horizontal and vertical displacements is available. To obtain such data, aerial stereophotogrammetry was applied to build 2-m resolution digital terrain models (DTMs) of HL at three epochs (1996, 1973, and 1952) (Dewitte et al. 2008). An additional DTM was interpolated from airborne LIDAR data acquired in 2002 by the Flemish Government (Fig. 20.5d) (Dewitte 2006; Dewitte et al. 2008). Simple DTM subtraction yielded direct estimates of the vertical displacement of each landslide pixel during the considered time interval with a confidence interval of ±0.75 m (Fig. 20.7).

Between 1952 and 1973 (Fig. 20.7a), the topographical changes were very limited. The main scarp remained unchanged. Small collapses observed at the head of the slide might have resulted from tension crack formation and destabilization in response to high groundwater levels at the contact with the Aalbeke clays, similar to what is currently observed in other landslides of the Flemish Ardennes. The role of runoff is poorly known. No field data are available and one even ignores whether runoff induced a net volume loss within the landslide, or rather transported sediment from above the main scarp. However, it was however probably of little importance, due to the presence of a forested zone upslope of the landslide head during this entire period (Dewitte 2006). The elongated zone of uplift observed along the Hekkebrug road north of house 2 actually represents improvement works that consisted in adding layers of stone bricks and asphalt to increase road accessibility (Van Den Eeckhaut et al. 2007a).

By contrast, significant movements occurred during the 1973–1996 period (Fig. 20.7b), revealing a typical rotational pattern, with a subsiding zone at the head, an intermediate area without vertical displacement, and an uplifted zone of accumulation towards the foot of the landslide. Immediately downslope of the main scarp, large values of apparent collapse, corresponding to the height of the scarp (~7 m), actually indicate a scarp retreat. The horizontal retreat can be approximated by the width of the band with collapsed terrain

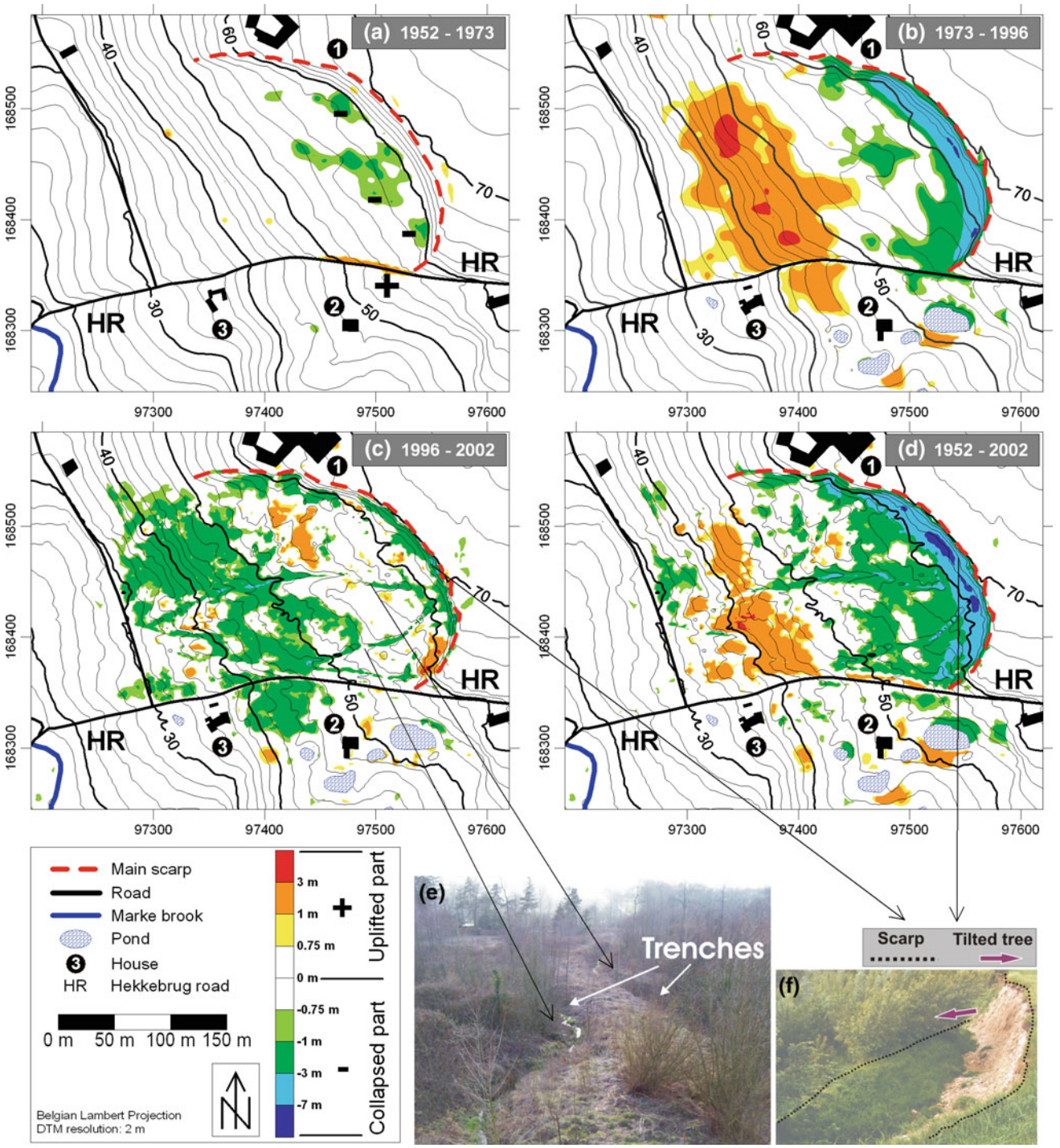

Fig. 20.7 Maps of vertical ground displacements within the Hekkebrugstraat landslide (landslide 1 in Fig. 20.4) inferred from DTM comparisons. **a** From 1952 to 1973; **b** from 1973 to 1996; **c** from 1996 to 2002; **d** from 1952 to 2002. In view **a** and **b**, the underlying contour lines describe the 1973 and 1996 topographies, respectively, whereas the 2002 topography is shown in views (**c**) and (**d**). Only vertical movements >1σ (0.75 m) uncertainty are represented. **e** West-looking view from the *top* of the main scarp of two 2-m-deep drainage ditches dug in 2000 (picture taken in February 2003). Young trees growing within the landslide are mainly poplar trees planted in place of their tall predecessors cut in September 1995 after the main reactivation. **f** Main scarp reactivation occurred in March 2002 showing clearly the listric geometry of the slip surface (picture taken in May 2002) (from Dewitte et al. 2008)

Fig. 20.8 Horizontal displacements measured within the Hekkebrugstraat landslide (landslide 1 in Fig. 20.4) between 1973 and 1996. **a** General view. **b** Focused view on wall displacements close to house 2. The areas collapsed and uplifted between 1973 and 1996 (see Fig. 20.7) are also represented (*grey* tones). The three photographs attest to traces of horizontal displacements (April 2004). (*A*) Picture taken from the Hekkebrug road upslope house 2. The backward toppling of the trees towards the landslide head is due to lateral displacement of the terrain. (*B*) Picture taken from the Hekkebrug road in front of house 2. The main entry, which originally faced the house, has moved several metres downslope since the February 1995 reactivation. (*C*) Picture taken on the road crossing the toe of the landslide. The backward toppling of the trees towards the landslide head is also due to lateral displacement of the terrain (from Dewitte et al. 2008) ▶

and reaches locally 15 m. Beyond artificial soil surface elevation changes around the ponds near house 2 (Fig. 20.7b and c) (Van Den Eeckhaut et al. 2007a), no area outside of the landslide shows significant height difference between the two models, thus validating the comparison.

Van Den Eeckhaut et al. (2007a) pointed out that ground movements during the 1973–1996 period were mainly due to the reactivation event of February 1995. This reactivation was triggered by heavy rainfall during the winter 1994–1995. In addition, the rain effect was further enhanced by increased surface runoff produced on bare cultivated areas upstream of the main scarp during that winter (Fig. 20.5c), resulting in an increase of the water volume flowing directly into the landslide zone. Moreover, the artificial loads brought by the improvement of the Hekkebrug road and the digging of several ponds close to house 2, and the absence of well-maintained drainage ditches after the cessation of the agricultural activities within the landslide zone in the 1950s contributed also to reactivations (Van den Eeckhaut et al. 2007a).

A decrease in landslide activity is observed after 1996 (Fig. 20.7c). This period is characterized by the subsidence of large areas within the landslide, mainly due to compaction upon drainage in response notably to the digging of two 2-m-deep ditches across the landslide area in 2000 (Fig. 20.5d, 20.7c, e). Starting from the base of the main scarp, these ~250-m-long ditches drain the spring water exfiltrating from the aquifer perched above the Aalbeke clays, and the runoff water (Dewitte et al. 2008). As a consequence, little displacement has been observed in the zone of accumulation since 2001 (Van Den Eeckhaut et al. 2007a). The main scarp, however, was still active during this period, as shown in Fig. 20.7f. A 25-m-long, 4-m-wide soil slice collapsed in March 2002. Soil material was also artificially removed and displaced within the landslide, explaining, e.g. the anomalous uplifted zone just downslope of the main scarp close to the Hekkebrug road. Figure 20.7d sums up the vertical soil surface displacements induced by the landslide reactivation and the main human interventions, mainly since February 1995.

The volume change of the landslide can be estimated from the comparison of the DTMs (Dewitte et al. 2008). According to this comparison, and after correction for the impact of road improvements, a volume loss of ca. 5000 ± 1000 m^3 was recorded between 1952 and 1973. Between 1973 and 1996, ca. $37{,}000 \pm 5000$ m^3 were lost in the upper part of the landslide, approximately balanced by the ca. $38{,}000 \pm 6000$ m^3 deposited downslope. From 1996 to 2002, a volume loss of ca. $35{,}000 \pm 6000$ m^3 was computed. Unless the LiDAR data are systematically biased, this volume loss, much larger than that calculated for the period 1952–1973, is likely to result mainly from natural and artificial compaction of the recently displaced soil and, to some extent, removal of material induced by the creation of the two longitudinal drains (Fig. 20.7c, e).

20.2.2.3 Horizontal Displacements

Horizontal ground displacements were measured both at the main scarp and within the landslide (Fig. 20.8) (Dewitte et al. 2008). As the main scarp is located at the border of a plateau, its retreat may be compared to a horizontal displacement, locally reaching 20 m between February 1995 and April 2006 (Fig. 20.8a). Obviously, this retreat did not result from a single reactivation affecting the whole scarp, but rather from successive collapses like that observed in 2002 (Fig. 20.7f).

The position of walls located between houses 2 and 3 was also measured in 1973 and 1996 (Fig. 20.8). Whereas the brick walls next to house 3 were not affected by the reactivation, the displacements of the walls in front of house 2 clearly testify to the downslope movement of this area (Fig. 20.8b). The displacements were in general larger along the road (Fig. 20.8b), i.e. closer to the centre of the moving mass, where the shear strength is smaller. Road displacements within the transfer area also bear witness to lateral motion (Fig. 20.8), but no control point is available to allow an accurate estimate of movement.

Topographic profiles are very illustrative of the combination of vertical and horizontal displacements (Fig. 20.9). Figure 20.9a shows that the main scarp retreat, amounting to 14 m in this profile, is clearly associated with the zone of the highest subsidence at the landslide head. According to the conceptual model developed by Casson et al. (2005) for rotational landslides, the distribution of the topographic variations between 1973 and 1996 corresponds to a large rotation angle dividing the landslide into three areas

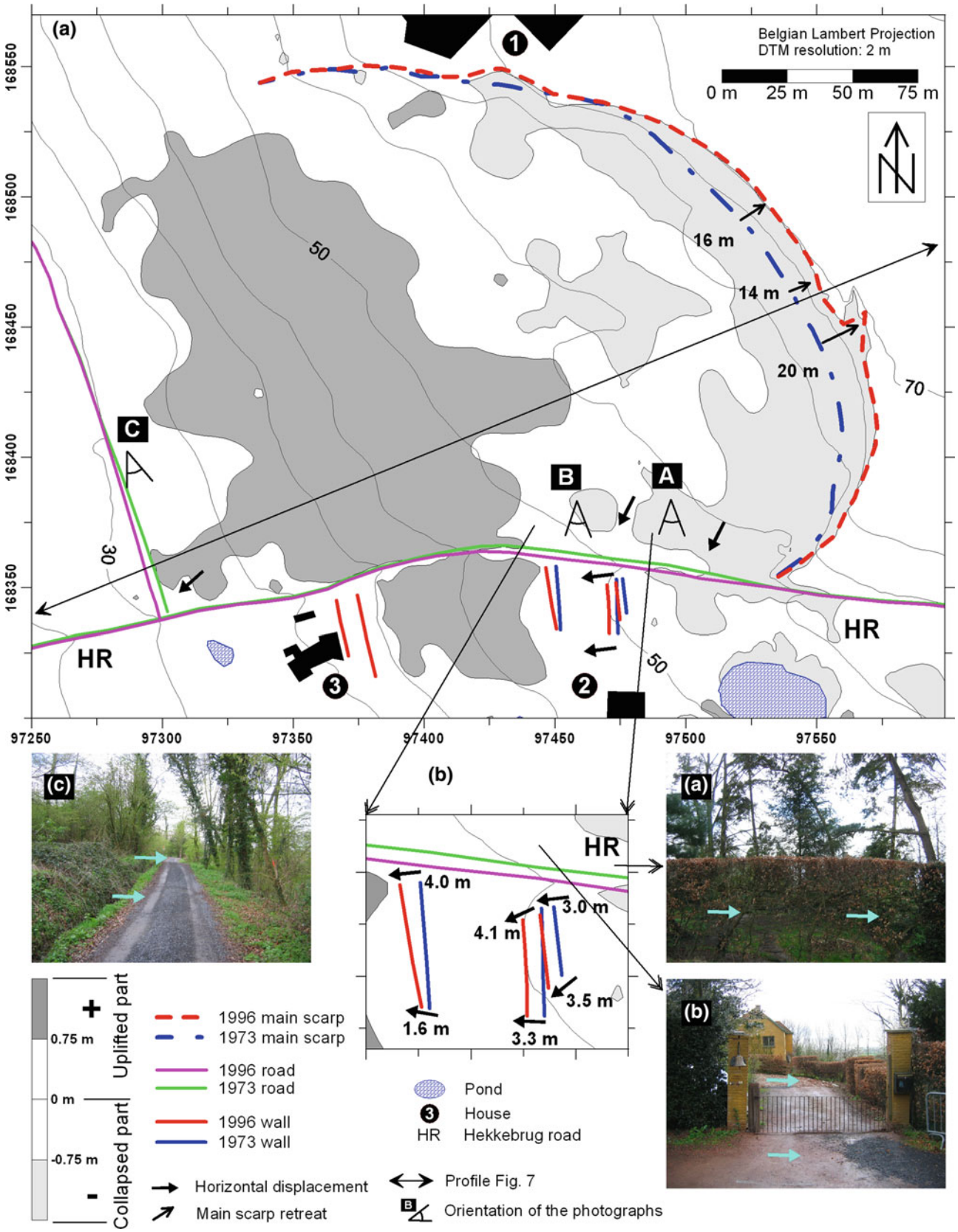
(a)
Belgian Lambert Projection
DTM resolution: 2 m
0 m 25 m 50 m 75 m
168550
168500
168450
168400
168350
97250
97300
97350
97400
97450
97500
97550
16 m
14 m
20 m
50
70
30
HR
A
B
C
(b)
(c)
4.0 m
3.0 m
4.1 m
3.5 m
1.6 m
3.3 m
+
0.75 m
0 m
-0.75 m
-
Uplifted part
Collapsed part
1996 main scarp
1973 main scarp
1996 road
1973 road
1996 wall
1973 wall
Pond
House
Hekkebrug road
Horizontal displacement
Main scarp retreat
Profile Fig. 7
Orientation of the photographs

(depletion–transfer–accumulation). The distribution of elevation changes within the profile 1973–1996, the shape of the visible part of the surface of rupture at the landslide head, and the alternation of subhorizontal clayey sand and clay layers suggest that the ~220-m-long surface of rupture of the February 1995 reactivation is situated at a depth of ~20 m (Fig. 20.9a), in contact with the Aalbeke clays. The uplift in the zone of accumulation is not a true vertical surface movement, but mainly the effect of the downslope lateral displacement of the slipped mass along the curved rupture surface (Fig. 20.9a). Likewise, the transfer area where no vertical displacement of the surface is observed between the collapsed and uplifted parts of the landslide corresponds to a zone of mainly horizontal motion. This model agrees with the values of lateral displacement measured at walls (Fig. 20.8b). The small uplifts measured in the landslide toe, downslope of the intersection between the lower part of the surface of rupture and the original ground surface (Fig. 20.9a), correspond with several small earthflows subsequent to the main reactivation (Van Den Eeckhaut et al. 2007a).

Another issue is whether this deep reactivation occurred along the pre-existing rupture surface of the original landslide or developed into the landslide debris. Electric

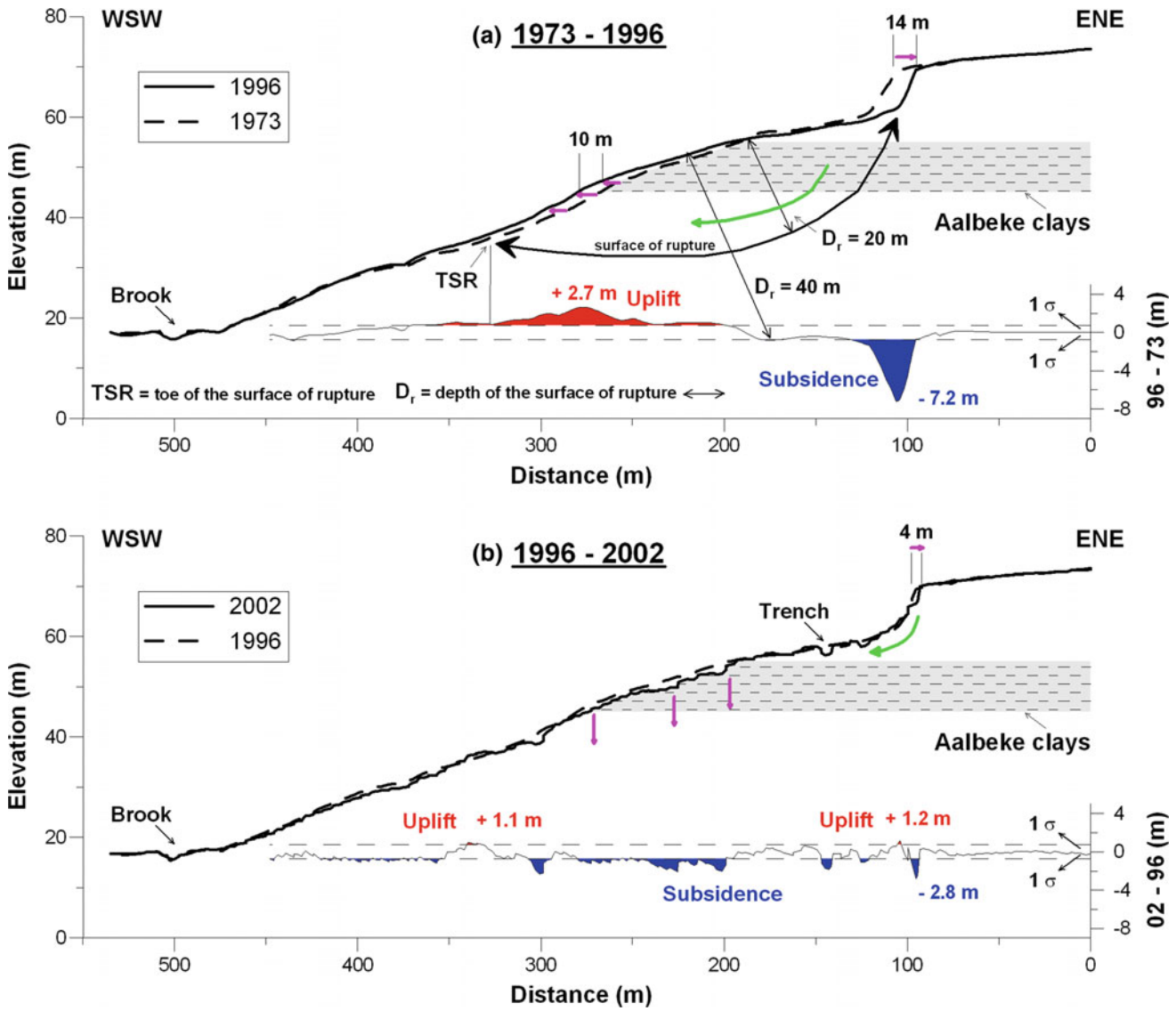

Fig. 20.9 DTM cross-sections of the Hekkebrugstraat landslide (landslide 1 in Fig. 20.4) compared with vertical displacement profiles (see location in Fig. 20.8). **a** Ground displacements between 1973 and 1996. **b** Ground displacements between 1996 and 2002. Lateral and vertical motions of the main scarps and ridges are represented by *horizontal* and *vertical purple arrows*, rotational motions by *curved green arrows*. In *blue* and *red*, associated profiles of the >1σ (0.75 m) vertical displacements obtained by DTM subtraction. Delimiting the collapsed and uplifted areas. Maximum and minimum vertical displacements are also provided (from Dewitte et al. 2008)

resistivity profile measurements carried out across a similar but dormant rotational earth slide revealed a surface of rupture at 15 m depth (Van Den Eeckhaut et al. 2007c), pretty similar to what is found for the HL reactivation, and also in contact with the sensitive clays of the Aalbeke Member (Fig. 20.9a). The Hekkebrugstraat landslide, as many others in the Flemish Ardennes and, in particular, the one studied by Van Den Eeckhaut et al. (2007c), is probably a multiple rotational slide, the original rupture surface of which was partly reused by the February 1995 reactivation. Assuming a 20 m depth of the surface of rupture, Dewitte et al. (2008) computed a landslide volume of ~625,000 m^3.

The 1996–2002 comparison of topographic profiles shows a succession of positive and negative vertical variations of topography (Fig. 20.9b). Until 2000 and the construction of the two drainage ditches, several flow-like reactivations affected the zone of accumulation (Van Den Eeckhaut et al. 2007a). Starting from the top, the first subsidence/uplift succession is due to the reactivation of the main scarp in March 2002 (e.g. Fig. 20.7f). According to the model of Casson et al. (2005), this profile corresponds to a small rotation angle, suggesting that the corresponding reactivation did affect the landslide only shallowly. Consequently, the zone of accumulation mainly underwent compaction and, locally, the effects of anthropogenic material displacements.

20.2.2.4 Reactivations and Other Displacements

The HL example aimed at providing a better understanding of the mechanisms and controlling factors of ground movements within old landslides. Dewitte et al. (2009) carried out such an analysis for the other 12 landslides located in Fig. 20.4. They showed that the setting and the magnitude of the displacements vary spatially and temporally. Within the most active landslides, the movement pattern is typically rotational deep-seated failure with subsidence in the zone of depletion and uplift within the zone of accumulation. However, a detailed analysis of the vertical and horizontal movements allowed them to recognize various slope processes and the related controlling factors. A distinction can be made between reactivation and non-reactivation features. Large reactivations affect the landslides in depth by reusing pre-existing surfaces of rupture. They are associated with the largest amounts of subsidence and uplift. Smaller reactivations are more confined and affect only the landslide head. These findings suggest an overall retrogressive activity of multiple rotational earth slides. Other measured displacements were produced by shallow planar slide-earthflows occurring in the zone of accumulation, sometimes as a consequence of a large reactivation, and small shallow failures occurring independently of the presence of the old landslides.

Most slope movements are triggered by intense rainfall. Among the factors that control their spatial and temporal distribution, vegetation clearly reduces the potential for shallow failures in the forested parts, due to an increase in shear strength via root cohesion and soil moisture abstraction during evapotranspiration, and anthropogenic activities alter the probability of movement occurrence.

These results support the hypothesis that slope movements affect the old landslides more frequently than suggested by the archive analysis. They stress the need for considering old landslides in land management and mitigation strategies in hilly areas, even if they seem stabilized at first glance.

On a final note, it should be mentioned that zones affected by landslides in the Flemish Ardennes are also often affected by soil piping and soil pipe collapses (Verachtert et al. 2010), which induce mean soil loss rates of 2.4–4.6 ton/ha/year (Verachtert et al. 2011). It is hypothesized that poorly drained landslides may create favourable conditions for pipe development (Verachtert et al. 2012). No field evidence was found that pipe development enhanced landsliding, probably because the subsurface drainage discharge generated upslope of the landslide and flowing through the pipes is too small. Even when pipes become blocked, it is more likely that new pipes develop and new pipe collapses occur than that they trigger or reactivate landslides. A conceptual model, summarizing all elements that influence piping erosion in the Flemish Ardennes, including the role of landslides, is presented by Verachtert et al. (2012).

20.3 Other Landslides in Belgium

Beyond the LiDAR-data-based mapping of landslides in the Flemish part of Middle Belgium (Van den Eeckhaut et al. 2011), several studies identified ancient and modern landslide features in a few places of the Meso-Cenozoic cover of Wallonia and the Grand-Duchy of Luxemburg (Ozer et al. 1998; Demoulin et al. 2003; Demoulin and Chung 2007; see also Chap. 23) and the recent LiDAR DTM of the Walloon region confirms and extends unpublished observations by A. Ozer that landsliding also affected the Permian fill of the graben of Malmédy in northern Ardenne (Mreyen et al. 2016). While modern landslide activity or reactivation in Middle Belgium has been addressed in the previous section, we will focus here on the origin of ancient deep-seated landslides in the Pays de Herve, eastern Belgium. Indeed, the limited modern landsliding phenomena caused by combined climatic and anthropogenic triggers in the most landslide-prone areas of Belgium (Flemish Ardennes, Pays de Herve) are in sharp contrast with the much larger size of the mapped old landslides in these areas, raising the question of a possible different origin of the latter.

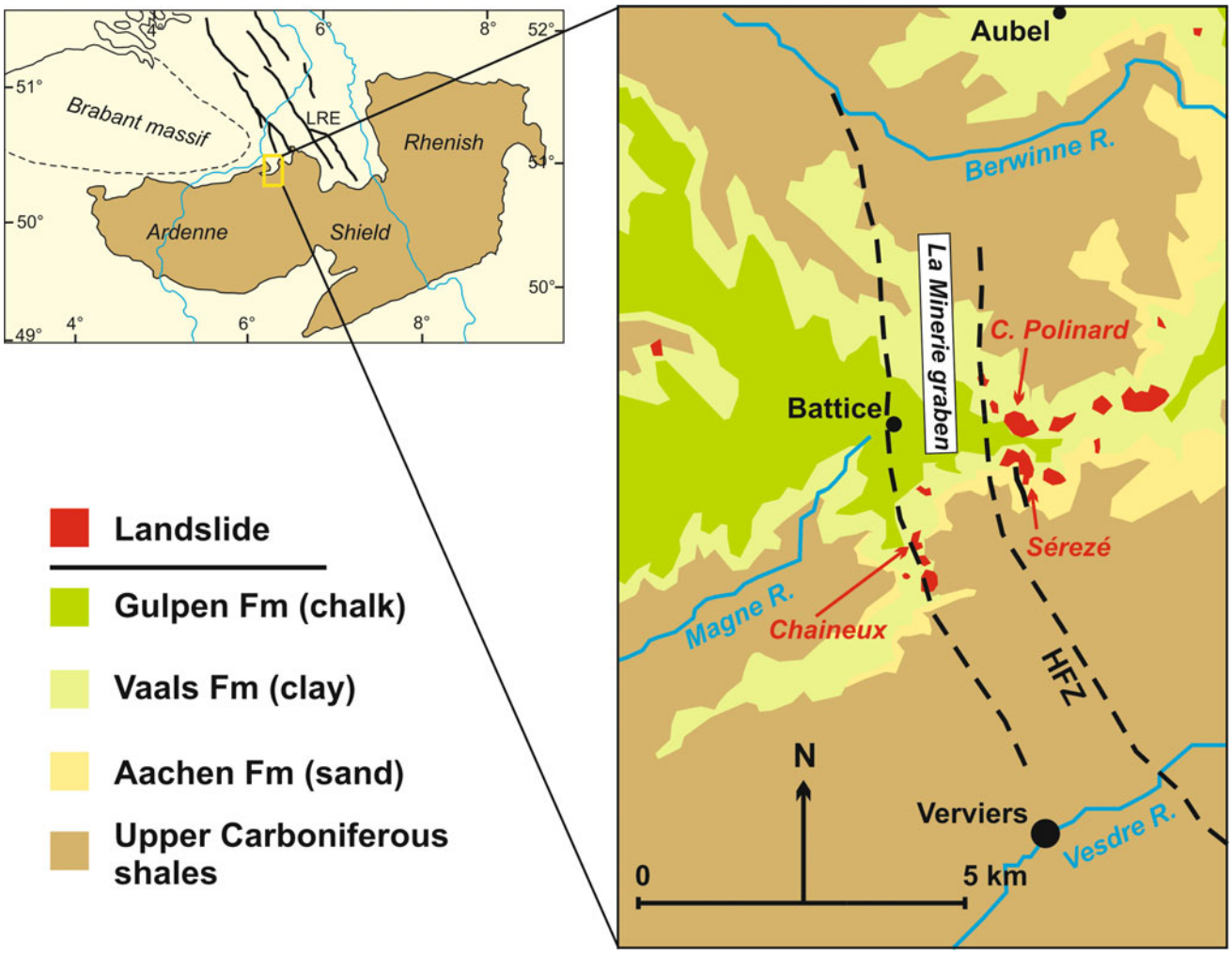

Fig. 20.10 Location map and simplified geology of the Pays de Herve in Belgium, showing also the landslide distribution within the study area, with the location of the Sérezé, Croix Polinard, and Chaineux landslides, described or mentioned in the text. *HFZ* Hockai fault zone

20.3.1 Geographical and Geological Settings

Geographically, the Pays de Herve is situated east of Liège and the Meuse valley, where it forms the easternmost part of the northern Ardennian foreland at altitudes between 200 and 350 m (Fig. 20.10). However, contrasting with the low plateaus of Middle Belgium, which are separated from the Ardenne itself by the intervening Condroz plateau and the Meuse valley, it is adjacent to the Ardennian margin and represents a kind of intermediate setting between Condroz, with which it shares its largely outcropping Paleozoic basement, and Hesbaye (or Haspengouw, in Flemish), similarly preserving an extended Cretaceous cover.

The geological and topographic contexts of landsliding in the Pays de Herve are fairly similar to those encountered in the Flemish Ardennes. The landslides affect poorly consolidated sediments of the Cretaceous cover that makes up the bulk of the ridges running across the Herve Plateau. These subhorizontal cover deposits rest on the Upper Carboniferous shales of the folded Paleozoic basement. The basal Aachen Formation is mainly comprised of fine sands interlayered with coarse sands and clays. Although the area where landslides are mapped corresponds to the westernmost extension of the formation, the sands are between 2–3 and 10 m thick. The overlying Vaals Formation displays glauconiferous clays and marls. Its maximum thickness is 25 m in the area affected by landslides. To the east, it gradually becomes sandier and contains indurated layers. Resting on the Vaals clays, the chalks of the Gulpen Formation are well preserved on top of most ridges of the Pays de Herve but are almost absent in the landslide zone. In their upper metres, they are generally weathered to clay-with-flints, frequently displaying solution pockets filled with remnants of Tertiary marine sands and Quaternary loess. The landslides are

essentially developed within the clays of the Campanian Vaals Formation but in close connection with the presence of the underlying Aachen sands.

While the WSW-striking Variscan thrust faults of the basement have been inactive for a long time, several NNW-striking Variscan faults were episodically reactivated as transtensional or pure normal faults during the Cenozoic. In particular, such active faults, and especially the Ostende fault, which represents the local segment of the seismogenic Hockai fault zone (see Chap. 13), define the small graben of La Minerie. Parallel to the nearby bounding faults of the Roer Valley Graben, the major Hockai fault zone runs across the main landslide cluster (Fig. 20.10).

Topographically, the Pays de Herve is a moderately dissected tableland with a relief of 80–100 m and slope angles rarely exceeding 12°. The landslides occur in the upper part of the slopes, most of them along the main E-W divide separating the Berwinne and Vesdre drainage basins, and a few others along a secondary ridge extending S and then WSW within the Vesdre basin (Fig. 20.10).

With respect to hydrogeology, the main aquifer of the Pays de Herve lies within the Gulpen chalks, but numerous small aquifers also exist within the Aachen sands, where they are trapped between the clays resulting from the Mesozoic weathering of the Palaeozoic basement, clay layers inside the Aachen Formation and the Vaals clays. Another aquifer is also present in the underlying fissured Palaeozoic shales. As for the climatic context, present-day yearly rainfall is 900 mm, and the centennial daily rainfall is of 99 mm at the Thimister station, right in the centre of the landslide zone.

20.3.2 Anatomy of the Sérezé Landslide

Extending over 12 ha, the Sérezé landslide is one of the largest and best representative of a set of 15 large landslides concentrated in an area of $\sim 5 \times 3$ km^2 in the south-central Pays de Herve (Fig. 20.10). Located on the southern slope of the main E–W ridge and facing to the southwest, it has a width of 550 m and extends on 250 m downslope of a 10 to 15-m-high head scarp. Though not recently activated, this double-arcuate scarp displays slopes between 17 and 22° that abruptly interrupt the gently sloping (by 8–9°) ridge flank in its upper part (Fig. 20.11). At its foot are several elongate tilted and rotated blocks with marked counterslopes that determine intervening depressions. As for the main part of the landslide body, it features a hummocky topography, especially in its lower half, and is terminated by a steep $\sim$2-m-high toe scarp. The great length of this body in comparison with that of the upslope rotated blocks suggests that a significant translational slide component is also present, making the Sérezé landslide a compound feature in the sense of Hutchinson (1988).

An electrical resistivity tomography (ERT) of the landslide, complemented by a series of electrical and seismic refraction soundings, was carried out in order to image its overall internal structure (Demoulin et al. 2003). Aided by the local lithostratigraphy known from borehole data, the tomographic analysis of the rock column upslope of the slide shows the superposition of a 5 to 10-m-thick moderately resistive upper layer corresponding to the slightly weathered chalks of the Gulpen Formation, then a $\sim$20-m-thick layer of very low resistivity, indistinctly including the Vaals clays and the underlying Aachen sands, and a basal layer of increasing resistivity representing the Paleozoic basement and featuring a possible steeply dipping fault (Fig. 20.12). Inside the landslide, deformation of the Vaals clays evidences at least two $\sim$25-m-thick rotated blocks whose bottom surface attests the listric shape of the basal shear in the upper half of the disturbed volume. By contrast, the downslope half of the landslide appears as a 10-m-thick slope-parallel body extending over 100 m and slightly thinning in its distal extremity. This landslide structure fully confirms the multiple rotational plus translational characters also inferred from the surface topography of the landslide.

A 20-m-long trench dug in the landslide toe, parallel to the slide direction, provided a detailed view of how the displaced material moved to accumulate and form the toe scarp. A second trench in another nearby landslide, shown in Fig. 20.13 with the ^{14}C ages obtained for three charcoal pieces, revealed a similar structure. At Sérezé, the original ground surface is identified by a podzolic soil developed on colluviated silts of mainly eolian origin. Superposing a grey humic horizon, a bleached eluviated horizon and a variegated illuvial horizon, this soil is $\sim$0.6-m-thick under the distal part of the toe scarp, then displays local bulging and thickening to >1 m before wedging and rapidly disappearing inward. The silts rest on 1 to 2-m-thick colluviated green glauconiferous Vaals clays that shallow auger borings showed lying over a thin ($\sim$0.3 m) bed of water-saturated purple sands of the Aachen Formation and Paleozoic schists weathered to black clay. Covering the soil and the colluviated material, the slipped masses are mainly made of light grey-brown clays with few flints and a subordinate silt component, a mixture of all sediments cropping out upslope. In contrast with the somewhat blurred contact surface between the undisturbed soil and the overlying slipped clays, an undulating sharp shear surface separates the latter in two distinct bodies, from which the lower one shows lumps of soil especially in its upper part. This exposed section suggests that, before leaving the soil on which it slid intact at the far end of its toe, the landslide, which had started several tens of metres upslope, partly scraped it, stacking broken soil

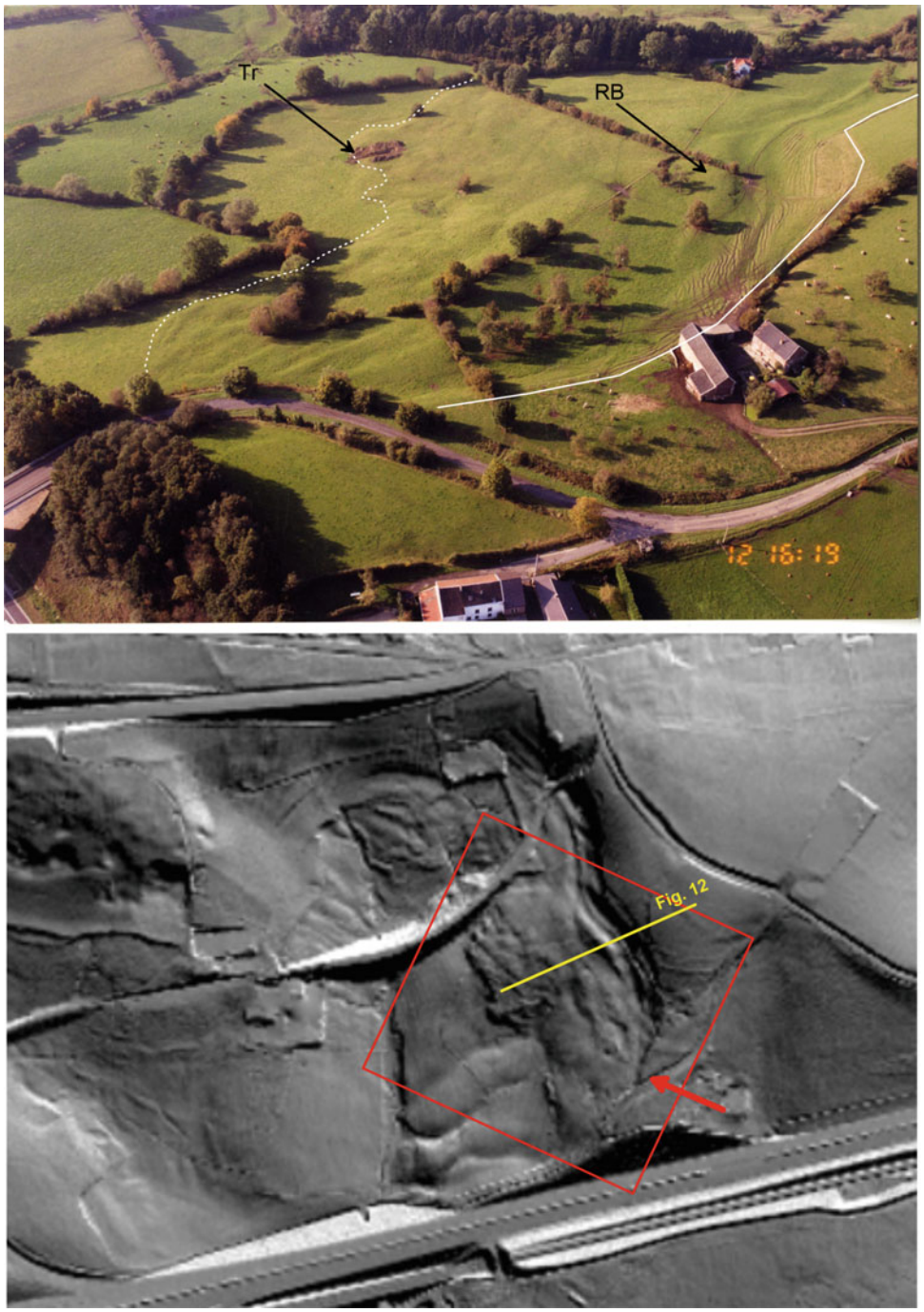

Fig. 20.11 The Sérezé landslide on the southern side of the main E–W ridge of the Pays de Herve (see location in Fig. 20.10). *Top* oblique aerial photograph of the southern part of the landslide. The *white line* denotes the *top* of the headscarp, the *dashed white line* follows the landslide toe. *RB* rotated block; *Tr* trench opened in the toe of the landslide. *Bottom* excerpt of the LiDAR DTM of Wallonia showing the general bilobate shape of the Sérezé landslide with two coalesced shear surfaces. The *red arrow* indicates the direction in which the photograph is looking, the *red rectangle* delimits the area covered by the photograph

pieces in a final bulge (Fig. 20.13). However, no positive field observation can resolve whether the two slipped bodies were emplaced simultaneously or during different slip episodes, except maybe that the lower one is, as a whole, strikingly more rubefied than the other.

Fortunately, numerous charcoal pieces present not only in the buried original soil but also in the soil patches at the top of the lower body allowed for ^{14}C dating. A similar situation was encountered in another trench cut across a second landslide, north of the ridge (Fig. 20.13). Multiple ^{14}C ages obtained in the two trenches have brought consistent insight into a common oldest time of landslide probable initiation between 50 and 250 AD, followed by several reactivation episodes in one or the other place around 400, 700, and 1250 AD (Fig. 20.14). In particular, these dates demonstrate that the upper body in the Sérezé landslide toe moved onto the lower one during a reactivation event in the thirteenth century.

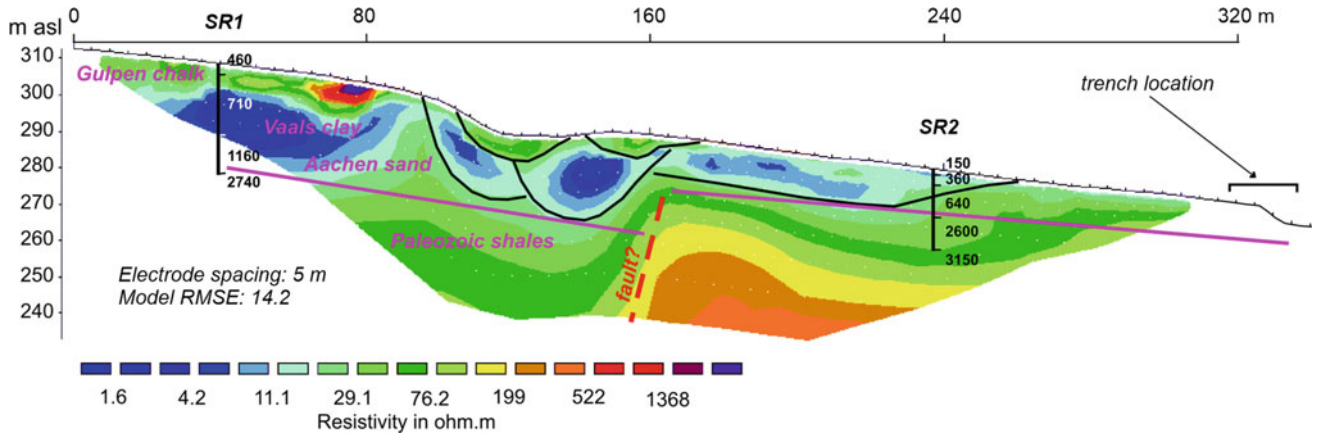

Fig. 20.12 Electrical resistivity tomography across the Sérezé landslide, with interpretation of the subsurface structures (see location on Fig. 20.11). *Underlined in black*, several rotated blocks are identified in the *upper part* of the landslide, whereas its *lower part* corresponds to a single translational unit. SR1 and SR2 are seismic refraction soundings with seismic velocity given in m/s. The *magenta lines* correspond approximately to the base of the Aachen Formation as it can be extrapolated upslope from its position in the trench, based on the observed resistivity and seismic velocity contrasts

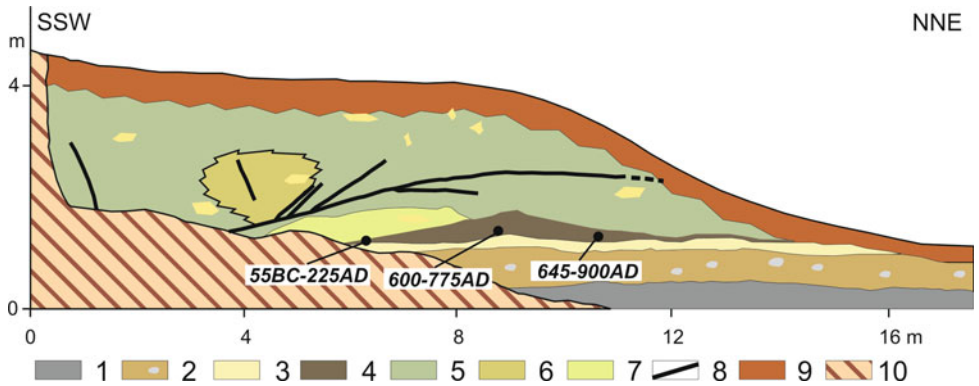

Fig. 20.13 Section across the toe of the Croix Polinard landslide on the north-looking side of the Battice ridge (see location on Fig. 20.10). *1* Paleozoic shales weathered to clay; *2* clay-with flint pre-landslide colluvium; *3*, *4* eluvial and humic horizons, respectively, of a podzolic soil developed in a silt of mainly eolian origin; note the bulging of the humic horizon in the centre of the section, with location of the ^{14}C-dated samples (calibrated 2σ ranges); *5*, *6*, *7* slipped masses, chiefly made of reworked Vaals clays with sparse sandstone blocks; *8* major shear surfaces; *9* present-day soil; *10* waste hiding the base of the section

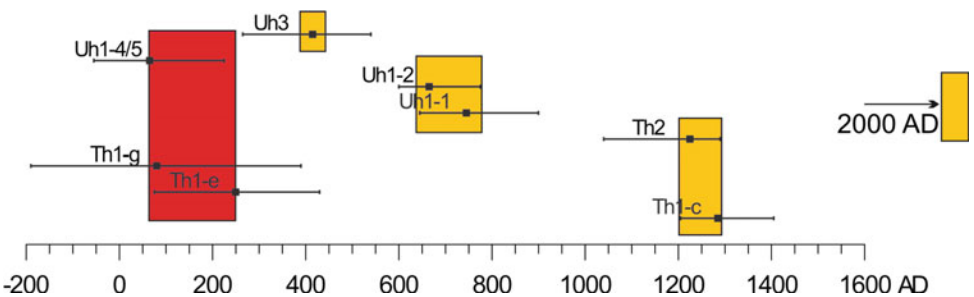

Fig. 20.14 ^{14}C date distribution (calibrated ages with 2σ range) of landslide motion in the Sérezé (Th) and Croix Polinard (Uh) landslides, and movements observed (1998 event) and monitored (1999–2005) in recent years. In *red*, assumed time period of landslide initiation; in *orange*, reactivation phases in either landslide

20.3.3 Mechanism and Causes of Landsliding in the Pays de Herve

20.3.3.1 Mechanism

The landslide surface topography, its ERT-revealed overall structure and the toe internal structure consistently stress the compound character of the Sérezé landslide and the translational movement that prevailed in its lower half. While all landslides affect mainly the Vaals clays, shallow geophysics and field data also show that the lower planar part of the basal shear is always located in the Aachen sands or at their interface with the overlying clays. Moreover, no landslide (except perhaps metre-scale shallow slides) is observed in the clays where the underlying Aachen sands are absent. Demoulin et al. (2003) identified therefore sand liquefaction as the primary process initiating the large deep-seated landslides of the Pays de Herve. Indeed, it has been long since laboratory measurements and field observation have shown that these sands are highly liquefiable (e.g. Graulich 1969). Sand liquefaction having initiated translational downslope motion of the Vaals clays, this in turn destabilized the upslope part of the hillside, causing successive rotational movements in a retrogressive way. A unique confirmation of this motion sequencing is provided by one landslide where only the initial mid-slope translation occurred, leaving a graben-like depression upslope of the displaced mass. This complex process can hardly be envisioned other than catastrophic, made of a sequence of fast movements caused by a sudden overwhelming trigger.

Slope stability analyses reached a similar conclusion (Demoulin et al. 2003). While the sand-clay interface dips ~0.8° NNW (the majority of landslides having occurred accordingly on N- or NW-facing slopes), they showed that, in static conditions, the safety factor (F_s, ratio of shear strength over stress along the shear surface) remains well in the stability domain for translational surfaces sloping by 4° even when the sediments are water-saturated. Likewise, in case of rotational motion along a listric slip surface, F_s comes close to instability only for highly improbable conditions of shear surface geometry and geotechnical properties of the sands, therefore suggesting that a very unusual trigger is required for impulsing large-scale landsliding.

20.3.3.2 Causes

Since no observation supports footslope sapping by river erosion or human interference as possible causes of initiation of the deep-seated landslides of the Pays de Herve around 50–250 AD, triggers of large-scale landsliding have been searched in either climatic circumstances or a seismic event (Demoulin et al. 2003). Key to the discussion was the contrast observed between the major event during which all large landslides occurred, moving tens to hundreds of metres, and the several reactivation episodes that seem in general to have affected only a part of the existing landslides and caused metre-scale displacements.

The best documented reactivation occurred in the autumn of 1998, when a more than centennial daily rainfall of 126 mm created a new 100-m-long, 1.5-m-high head scarp and caused 1 m downslope displacement of part of an existing landslide that underwent anthropogenic perturbation since three decades at Manaihan (Demoulin and Glade 2004) (Fig. 20.10). Beyond this, this event barely provoked a few small ground cracks within the scarps of some of the other old landslides in the area. Continued monitoring of the destabilized Manaihan landslide showed that the persisting human-induced high pore-water pressures within the landslide body involved annual displacements in the order of 0.15–0.25 m year^{-1} taking place essentially at the end of the winter season, while extremely wet summer months (e.g. 288 mm in July 2000) were largely unable to cause ground motion (Demoulin 2006). In other words, such a rainfall event was unable even to significantly reactivate existing landslides in natural conditions. Likewise, two of the ^{14}C-dated reactivation episodes occurred around 700 and 1250 AD, two periods that various proxies (palynology, lake levels, testate amoebae) identify as especially wet, with cool wet winters, in NW Europe (Hendon et al. 2001; Holzhauser et al. 2005; Magny 2013), and they were nevertheless barely capable of inducing metre-scale displacements in some pre-existing landslides.

This strongly suggests that, although initiation of the large landslides occurred during another comparatively wet period, at least in west-central Europe (Holzhauser et al. 2005; Magny 2013), a period that in any case slightly postdates the wettest, highly landslide-prone, beginning of the Subatlantic (~2.8–2.0 ka cal BP: van Geel et al. 1996; Dikau and Schrott 1999; Chambers et al. 2010), a climatic trigger is certainly insufficient to explain such a major landsliding event. While this negative evidence is the first hint of a seismic origin of the landslides of the Pays de Herve, several positive arguments that together satisfy most criteria defined by Crozier (1992) to view landslides as earthquake-triggered convincingly support this interpretation too. These arguments are:

- All available data point to the dated landslides having been initiated simultaneously. Though not decisive and needing confirmation by dating further landslides, this is a necessary condition in order to consider a seismic trigger.
- The spatial distribution of the landslides cannot be explained on the basis of geological (rock type) or geomorphological (slope) conditions. By contrast, it is tightly linked to the Ostende fault, a segment of the

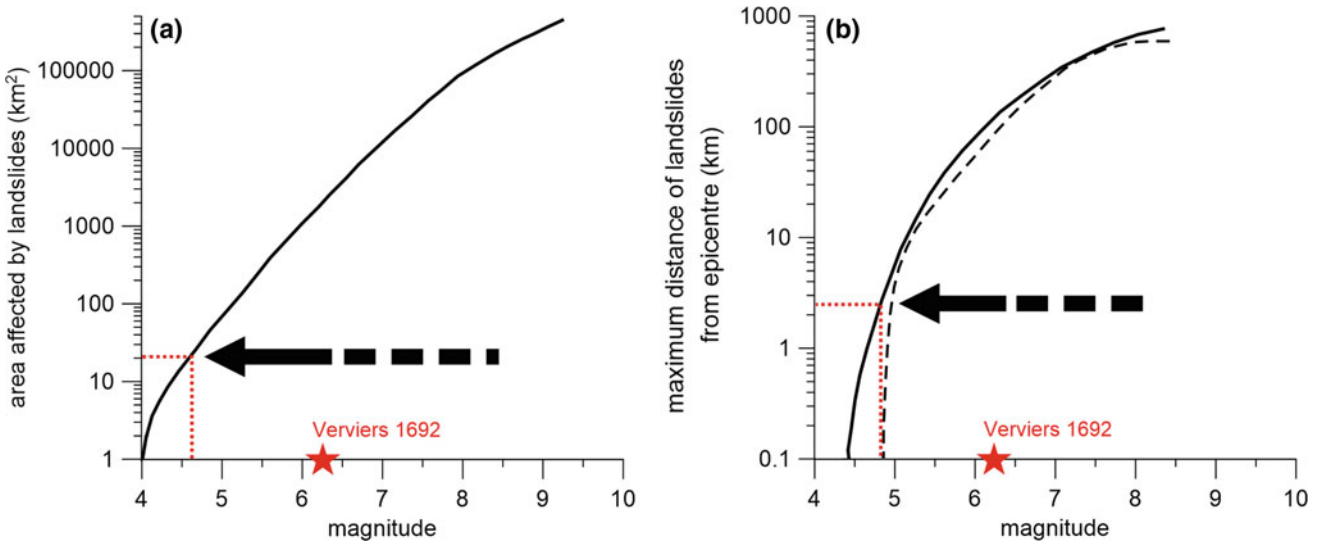

Fig. 20.15 Position of the Pays de Herve landsliding event within the empirical relationships between magnitude of the triggering earthquake and characteristics of the landslide distribution (**a** total area affected by landslides; **b** maximum distance of landslides from epicentre) in case of a seismic origin of the landslides (Keefer 1984). In **b**, the *solid curve* refers to 'coherent slides' and the *dashed curve* to 'lateral spreads' (and liquefaction-induced mass movements). Both relations point consistently to a possible M_L 4.5–5.0 earthquake (*red dotted lines*). The *red stars* locate the Verviers 1692 earthquake, which, based on the available data, seems to have been unable to cause landsliding in the study area

active Hockai fault zone in an area whose ongoing seismic activity is demonstrated (see Chap. 13) (Fig. 20.15).

- Stability analyses showed there is very little probability that the slopes be destabilized and cause extended landsliding in static conditions, even in the case of saturated sediments. A dynamic trigger was most likely, either seismic or possibly related to a catastrophic intense rainfall event at the hour-to-day scale.
- Liquefaction, which was the primary cause for setting the ground in motion, is in most cases associated with the dynamic oscillations of saturated sediments at the passage of seismic waves.
- The size characteristics of the landslides and their position in the upper part of gently sloping hillsides are typical of earthquake-triggered landslides.

Finally, if one admits the seismic origin of extended landsliding in the Pays de Herve in the period 50–250 AD, a concluding remark is that no exceptional earthquake was required to produce the observed set of deep-seated landslides. According to the empirical relationships between earthquake magnitude and different characteristics of the landslide distribution (maximum distance from fault rupture zone, total area affected by landsliding) established by Keefer (1984), and assuming that the seismic source was indeed the Ostende fault, an M_S 4.7–5.0 earthquake would have sufficed to cause their observed distribution. The same author also noted that the landslide type present in the Pays de Herve, i.e. coherent soil block slide, has been described in relation with earthquakes of magnitude M_S as low as 4.5. Such estimates are consistent with seismic hazard assessments for the area, which yield a return period of 447 years for an M_S 5.0 earthquake (Leynaud et al. 2000).

20.4 Conclusions

Through two representative examples, we provided insight into the landslide processes that are the most specific for Belgium. Even though the literature that focuses on these case studies is fairly abundant, we also showed that the understanding of these landslides is still suffering from several gaps, in particular when it comes to the timing of initiation and the factors at play at that moment. In the two cases, all available data suggest that major landsliding was caused by extreme events linked to former climatic and/or seismic conditions.

Although the landslides had an origin in natural environmental conditions, their recent dynamics, dominated by reactivation of ancient features, highlights the interactions with anthropogenic activities. This is demonstrated by using detailed qualitative analysis of information on landslide history and land-use changes provided by local inhabitants, aerial photographs and newspaper articles and internal reports, coupled with quantitative analysis.

In the regions west of Brussels (Fig. 20.2), we focused on landslides in Flanders. However, the geological and topographic settings typical of the Flemish Hills extend also in W Wallonia, and similar landslides are found there

as well (Ozer et al. 1998). Likewise, despite an apparently much contrasted general landscape, the same underlying landslide-prone conditions also characterize the landsliding area of the Pays de Herve in eastern Belgium.

The information presented here is not meant to be static. The wide range of LiDAR derivative products has recently become a powerful tool in landslide research, particularly for landslide identification and landslide inventory mapping (Jaboyedoff et al. 2012; Guzzetti et al. 2012). Recently, the first analysis of new high-resolution LiDAR data for the hilly regions south of the Flemish hills revealed new old-landslide features (Akkermans 2014). Similarly, the LiDAR DTM of Wallonia, available since 2015, already allowed for the identification of previously unknown landslides in the Malmédy area (Mreyen et al. 2016), while even the Ardennian slopes cut in Lower Devonian shales are not devoid of local landsliding (R. Maquil, oral communic.).

Finally, landslides themselves are dynamic features responding rapidly to all kinds of change. The reader visiting Belgian landslides with this book in hand will have to remember that most results presented here are from studies carried out in the early 2000s and much may have changed since then.

References

Akkermans B (2014) Grondverschuivingen in de Henegauwse en Waals-Brabantse Leemstreek. Unpublished thesis, Master of Science, Geography, KU Leuven—VU Brussel

Camelbeeck T (1993) Introduction à l'étude des tremblements de terre. La séismicité en Belgique et dans le nord de la France. Annales de la Société Géologique du Nord, T. 2 (2ème série) 5–22

Casson B, Delacourt C, Allemand P (2005) Contribution of multi-temporal remote sensing images to characterize landslide slip surface—application to the La Clapiere landslide (France). Nat Hazards Earth Syst Sci 5:425–437

Chambers F, Daniell J, ACCROTELM Members (2010). Peatland archives of late-Holocene climate change in northern Europe. PAGES News 18:4–6

Crosta GB, Frattini P, Agliardi F (2013) Deep seated gravitational slope deformations in the European Alps. Tectonophysics 605:13–33. doi:10.1016/j.tecto.2013.04.028

Crozier M (1992) Determination of paleoseismicity from landslides. In: Bell D (ed) Landslides (Glissements de terrain), proceedings 6th international symposium, vol 2, pp 1173–1180

Cruden DM, Varnes DJ (1996) Landslide types and processes. In: Turner AK, Schuster RL (eds) Landslides: investigation and mitigation, pp 36–75. Special report 247. Transportation Research Board National Research Council, National Academy Press, Washington, DC

DEM of Flanders (2007) Digital elevation model of Flanders (obtained by laser scanning). http://www.gisvlaanderen.be/gis/diensten/geo-vlaanderen/?catid=82007

Demoulin A (2006) Monitoring and mapping landslide displacements: a combined DGPS-stereophotogrammetric approach for detailed short- and long-term rate estimates. Terra Nova 18:290–298

Demoulin A, Chung C-J (2007) Mapping landslide susceptibility from small datasets: a case study in the Pays de Herve (E Belgium). Geomorphology 89:391–404

Demoulin A, Glade T (2004) Recent landslide activity in Manaihan, East Belgium. Landslides 1:305–310. doi:10.1007/s10346-004-0035-z

Demoulin A, Pissart A, Schroeder C (2003) On the origin of late Quaternary palaeolandslides in the Liege (E Belgium) area. Int J Earth Sci 92:795–805

Dewitte O (2006) Kinematics of landslides in the Oudenaarde area and prediction of their reactivation: a probabilistic approach. Unpublished PhD thesis, University of Liege

Dewitte O, Demoulin A (2005) Morphometry and kinematics of landslides inferred from precise DTMs in West Belgium. Nat Hazards Earth Syst Sci 5:259–265

Dewitte O, Chung C-J, Demoulin A (2006) Reactivation hazard mapping for ancient landslides in West Belgium. Nat Hazards Earth Syst Sci 6:653–662

Dewitte O, Jasselette JC, Cornet Y, Van Den Eeckhaut M, Collignon A, Poesen J, Demoulin A (2008) Tracking landslide displacements by multi-temporal DTMs: a combined aerial stereophotogrammetric and LIDAR approach in western Belgium. Eng Geol 99:11–22

Dewitte O, Van Den Eeckhaut M, Poesen J, Demoulin A (2009) Decadal-scale analysis of ground movements in old landslides in western Belgium. Zeitschrift für Geomorphol 53:23–45

Dewitte O, Chung CJ, Cornet Y, Daoudi M, Demoulin A (2010) Combining spatial data in landslide reactivation susceptibility mapping: a likelihood ratio-based approach in W Belgium. Geomorphology 122:153–166

Dikau R, Schrott L (1999) The temporal stability and activity of landslides in Europe with respect to climatic change (TESLEC): main objectives and results. Geomorphology 30:1–12

Graulich JM (1969) La géologie de l'autoroute Liège-Aachen entre Herve et La Saute (Clermont). Professional paper service Géologique de Belgique 5, 61 p

Günther A, Van Den Eeckhaut M, Malet J-P, Reichenbach P, Hervás J (2014) Climate-physiographically differentiated Pan-European landslide susceptibility assessment using spatial multi-criteria evaluation and transnational landslide information. Geomorphology 224:69–85. doi:10.1016/j.geomorph.2014.07.011

Guzzetti F, Mondini AC, Cardinali M, Fiorucci F, Santangelo M, Chang KT (2012) Landslide inventory maps: new tools for an old problem. Earth Sci Rev 112:42–66. doi:10.1016/j.earscirev.2012.02.001

Hendon D, Charman D, Kent M (2001) Palaeohydrological records derived from testate amoebae analysis from peatlands in northern England: within-site variability, between-site comparability and palaeoclimatic implications. The Holocene 11:127–148

Holzhauser HP, Magny M, Zumbühl H (2005) Glacier and lake-level variations in west-central Europe over the last 3500 years. The Holocene 15:789–801

Hutchinson J (1988) Morphological and geotechnical parameters of landslides in relation to geology and hydrology, General Report. In: Bonnard C (ed) Landslides, Proceedings 5th international symposium on landslides, vol 1, pp 3–35

IAEG Commission on Landslides (1990) Suggested nomenclature for landslides. Bull Int Assoc Eng Geol 41:13–16

Jaboyedoff M, Oppikofer T, Abellán A, Derron M, Loye A, Metzger R, Pedrazzini A (2012) Use of LIDAR in landslide investigations: a review. Nat Hazards 61:5–28

Jacobs P, De Ceukelaire M, De Breuck W, De Moor G (1999) Text clarifying the Belgian geological Map, Flemish Region, Map Shet 29 Kortrijk, Map Scale 1/50,000 (in Dutch). Ministerie van Economische Zaken and Ministerie van de Vlaamse Gemeenschap

Keefer D (1984) Landslides caused by earthquakes. Geol Soc Am Bull 95:406–421

Leynaud D, Jongmans D, Teerlynck H, Camelbeeck T (2000) Seismic hazard assessment in Belgium. Geologica Belgica 3:67–86

Magny M (2013) Orbital, ice-sheet, and possible solar forcing of Holocene lake-level fluctuations in west-central Europe: a comment on Bleicher. The Holocene 23:1202–1212

Mreyen A, Havenith H, Fernandez-Steeger T (2016) Geophysical investigation of landslides and fault scarps in the Hockai Fault Zone, Belgium. Geophys Res Abstr 18:2350

Ost L, Van Den Eeckhaut M, Poesen J, Vanmaercke-Gottigny MC (2003) Characteristics and spatial distribution of large landslides in the Flemish Ardennes (Belgium). Zeitschrift für Geomorphol 47:329–350

Ozer A, Bonino E, Closson D, Ozer P, Petit F, Pissart A (1998) Etude des contraintes physiques et géotechniques du Mont-de-l'Enclus. Convention DGATLP-ULG. Laboratoire de Géomorphologie et de Télédétection. Rapport final, 87 p

Somville O (1939) Le tremblement de terre belge du 11 juin 1938. Annales de l'Observatoire Royal de Belgique, 3^{e} série 2(5):273–287

Van Den Eeckhaut M, Poesen J, Verstraeten G, Vanacker V, Moeyersons J, Nyssen J, van Beek LPH (2005) The effectiveness of hillshade maps and expert knowledge in mapping old deep-seated landslides. Geomorphology 67:351–363

Van Den Eeckhaut M, Vanwalleghem T, Poesen J, Govers G, Verstraeten G, Vandekerckhove L (2006) Prediction of landslide susceptibility using rare events logistic regression: a case-study in the Flemish Ardennes (Belgium). Geomorphology 76:392–410. doi:10.1016/j.geomorph.2005.12.003

Van Den Eeckhaut M, Poesen J, Dewitte O, Demoulin A, De Bo H, Vanmaercke-Gottigny MC (2007a) Reactivation of old landslides: Lessons learned from a case-study in the Flemish Ardennes (Belgium). Soil Use Manag 23:200–211. doi:10.1111/j.1475-2743.2006.00079.x

Van Den Eeckhaut M, Poesen J, Verstraeten G, Vanacker V, Nyssen J, Moeyersons J, van Beek LPH, Vandekerckhove L (2007b) Use of LIDAR-derived images for mapping old landslides under forest. Earth Surf Process Land 32:754–769

Van Den Eeckhaut M, Verstraeten G, Poesen J (2007c) Morphology and internal structure of a dormant landslide in a hilly area: the Collinabos landslide (Belgium). Geomorphology 89:258–273

Van Den Eeckhaut M, Muys B, Van Loy K, Poesen J, Beeckman H (2009a) Evidence for repeated re-activation of old landslides under forest. Earth Surf Process Land 34:352–365. doi:10.1002/esp.1727

Van Den Eeckhaut M, Reichenbach P, Guzzetti F, Rossi M, Poesen J (2009b) Combined landslide inventory and susceptibility assessment based on different mapping units: an example from the Flemish Ardennes, Belgium. Nat Hazards Earth Syst Sci 9:507–521. doi:10.5194/nhess-9-507-2009

Van Den Eeckhaut M, Poesen J, Gullentops F, Vandekerckhove L, Hervás J (2011) Regional mapping and characterisation of old landslides in hilly regions using LiDAR-based imagery in Southern Flanders. Quat Res 75:721–733. doi:10.1016/j.yqres.2011.02.006

Van Den Eeckhaut M, Kerle N, Poesen J, Hervás J (2012) Geomorphology object-oriented identification of forested landslides with derivatives of single pulse LiDAR data. Geomorphology 173–174:30–42. doi:10.1016/j.geomorph.2012.05.024

Van Geel B, Buurman J, Waterbolk H (1996) Archaeological and paleoecological indications of an abrupt climate change in The Netherlands, and evidence for climatological teleconnections around—2650 BP. J Quat Sci 11:451–460

Verachtert E, Van Den Eeckhaut M, Poesen J, Deckers J (2010) Factors controlling the spatial distribution of soil piping erosion on loess-derived soils: a case study from central Belgium. Geomorphology 118:339–348

Verachtert E, Maetens W, Van Den Eeckhaut M, Poesen J, Deckers J (2011) Soil loss due to piping erosion. Earth Surf Proc Land 36:1715–1725

Verachtert E, Van Den Eeckhaut M, Poesen J, Deckers J (2012) Spatial interaction between collapsed pipes and landslides in hilly regions with loess-derived soils. Earth Surf Proc Land 38:826–835

Vranken L, Van Turnhout P, Van Den Eeckhaut M, Vandekerckhove L, Poesen J (2013) Economic valuation of landslide damage in hilly regions: a case study from. Sci Total Environ 447:323–336

Vranken L, Vantilt G, Van Den Eeckhaut M, Vandekerckhove L, Poesen J (2014) Landslide risk assessment in a densely populated hilly area. Landslides 12:787–798. doi:10.1007/s10346-014-0506-9